PHILOSOPHICAL TRANSACTIONS OF THE ROYAL SOCIETY A MATHEMATICAL, PHYSICAL & ENGINEERING SCIENCES

Key Issues in Image Understanding in Remote Sensing [and Discussion]

J.-P. A. L. Muller, J. C. Scott and S. Quegan

Phil. Trans. R. Soc. Lond. A 1988 **324**, 381-395
doi: 10.1098/rsta.1988.0027

Phil. Trans. R. Soc. Lond. A **324**, 381–395 (1988)
Printed in Great Britain

Key issues in image understanding in remote sensing

By J.-P. A. L. Muller

Department of Photogrammetry and Surveying, University College London, Gower Street, London WC1E 6BT, U.K.

Remotely sensed images of a planet's atmosphere, oceans and surface contain a plethora of confusing signals about the physical nature of these phase states. Historically, there has been an emphasis on the semi-automated extraction of feature classes based on the spectral properties of objects viewed within a scene and on the use of *ad hoc* manual photointerpretation techniques. Although these approaches will remain important, they are inadequate, on grounds of speed, accuracy and cost, for the increasing demands of data-gatherers and consumers.

Research has recently begun into the automation of image-interpretation tasks and the development of parallel machines with the required processing capabilities. Three important requirements are: (i) means to simulate the appearance of a scene, including the interaction of electromagnetic radiation with the surface and the effects of any intervening atmosphere; (ii) an understanding of how knowledge can be captured and introduced at different levels in the processing hierarchy and (iii) the application of constraints based on a knowledge of the geometry of objects in the scene. These three aspects will be illustrated by examples from various fields, including petroleum exploration, measurement of fluid motion and the extraction of digital terrain elevation models.

1. Introduction

Image understanding is concerned with the recovery of physical properties of a scene from image features and the computational systems that interpret images (see, for instance, Levine 1978; Tenenbaum *et al.* 1980; Marr 1982; Herman & Kanade 1986; Tailor *et al.* 1986). Remote sensing involves the extraction of physical properties of fluids or solids and their interpretation for a specific application end use, such as cartography (Doyle 1982) or climatology (Bretherton 1985). Image understanding in remote sensing is defined here as the development of techniques and computational systems for the automated extraction of scene properties from satellite and aerial imagery for specialist domains.

Requirements for such an automated extraction system arise from the increasing demands of data consumers (see, for instance, Goetz *et al.* 1983; Conway & Browning, this symposium) for more objective and quantitative information promised by a new generation of optoelectronic and microwave digital data gatherers (see, for instance, Goetz *et al.* 1985). Remotely sensed imagery is also believed to have a potential major role in spatial information systems under current development for geographical and environmental applications (see, for instance, Jackson, this symposium).

Automation has long played a role in the processing of satellite imagery (see, for instance, Jones & Colombeski 1981). However, the tendency has been to restrict automation to either preprocessing tasks, requiring a minimum of knowledge external to the image (e.g. associated telemetry-based estimates of the satellite position), or to crude attempts to force correspondence

between image patterns (e.g. cloud-tracking with pairs of geolocated geostationary satellite images: see, for instance, Morgan 1979). The degree of automation has frequently been a function of the perceived needs for volatile operational products and the efficiency of machine processing compared with human manual intervention. Examples include the production of cloud images for weather forecasting and, in the field of Earth resources, the use of *Landsat* data in the LACIE system for wheat-harvest monitoring and forecasting (NASA 1979).

The LACIE system is a prime example for a new trend in remote sensing, that of trying to create a combined information processing system, based upon a desire to understand physical processes. It included some degree of automation in the production of wheat-field coverage from classified images (by using manually selected training sets in the original multispectral images) and the application of knowledge external to the image (for instance, contemporary weather data) to predict harvest yield. This system was criticized for the lack of site-specific information (Swain 1985) but was the first major application of remote sensing applied to earth resources that used computer analysis for very large areas.

2. Limitations of current techniques

Current practice in geographical applications of remote sensing still relies heavily on the use and further development of statistical procedures (e.g. supervised or unsupervised classification of multispectral data) to try to extract information on surface cover based upon an attempt to separate ground-cover types by their spectral signature, even though there have been strong arguments advanced against its continued use (see, for example, Tenenbaum *et al.* 1980; Gerstl & Simmer 1986).

It is now widely recognized that multispectral classification has a number of severe shortcomings (Swain 1985); these include the following.

Signature extension. There is difficulty in extrapolating local spectral characteristics to larger geographic areas; this is both a sampling problem and a fundamental limitation in the use of laboratory spectral data in the field.

Mixture pixels. Every satellite-image pixel is likely to have more than one ground-cover type within the pixel's field of view.

Signature confusion. The atmosphere and the surface slope (see §3.3.) contribute part of the radiance recorded in every pixel.

Signature ambiguity. Owing to technological constraints (see Goetz *et al.* 1985) spectral bandpasses of sensor channels are frequently too broad to differentiate between ground-cover types (see Bernstein (1986) for a justification of *Landsat* Thematic Mapper band selection and Gerstl & Simmer (1986) for a critique of the severe limitations of relying on spectral signature for vegetation type discrimination).

Temporal instability. Multitemporal classified satellite imagery is both a function of signature confusion (namely the atmospheric conditions change over time) and the observation that spectral signatures for many ground cover types (namely vegetation) change over the time period between satellite overflights.

The difficulties of correcting for geometrical instabilities of aircraft have severely restricted the operational application of digital sensor technology to environmental monitoring. However, the use of aerial photographic data, begun in 1859 with Gaspard Tournachon's balloon-based observations, has continued unabated until now. Photogrammetric techniques (see, for in-

PHILOSOPHICAL TRANSACTIONS OF THE ROYAL SOCIETY A MATHEMATICAL, PHYSICAL & ENGINEERING SCIENCES

stance, Slama 1980) have been developed to correct for geometrical distortions associated with aerial photography, permitting manual stereo measurements of plan and elevation to be made with accuracies greater than 1 part in 10000 of flying height (Slama 1980). However, although computer assistance is now given in analytical plotters to permit online computation of geometry, little if any automation has been introduced into either the manual stereo measurement or the manual photointerpretation process. A notable exception for the latter is the combined use of map-derived data with digitized photographs (given a good camera model) in automated aerial image interpretation (see McKeown *et al.* 1985). However, this process still relies on the manual determination of the camera geometry.

Given this context, this paper attempts to present a radically different approach based on recent advances in machine vision. We address the question of what the key components of an image-understanding system are and report on recent results to develop these components using advances in computer graphical techniques, data structures and parallel processing technology.

3. Key components

3.1. *System architecture*

A simplified diagram is shown in figure 1 of the key components of a hypothetical image-understanding system in remote sensing. Missing from this diagram are explicit indications of the possible data flows and the invocation of (implicit) knowledge sources (see later).

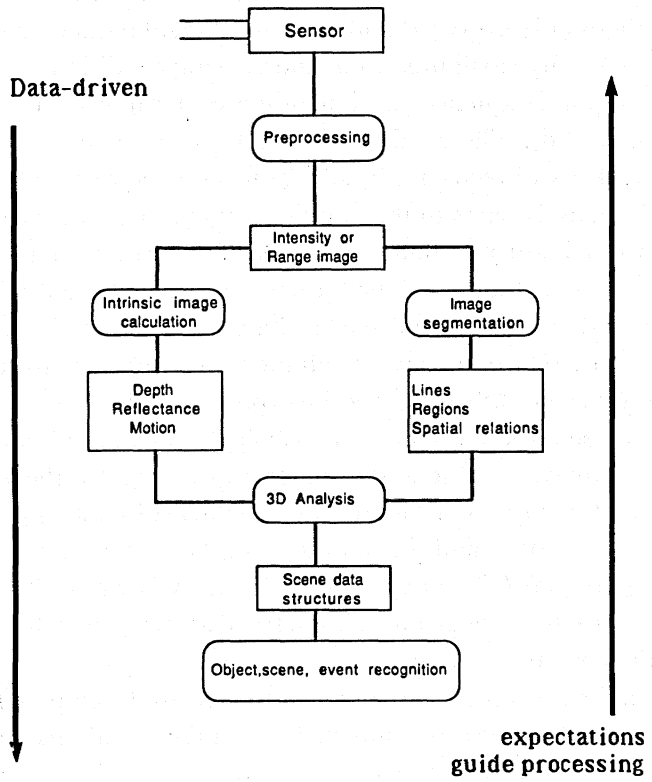

Figure 1. Key components of an image-understanding system for remote sensing. Such a system can be developed either for bottom-up control or the use of expectations to guide processing. Crucial features of such systems are the incorporation of three-dimensional information and the attempt to include knowledge about the image formation process.

There are two basic modes of operation of the system, commonly referred to as bottom-up or data-driven (i.e. from the sensed data to a scene description) and top-down or expectations-guide-processing (i.e. search for a specific instantiation of a physical object(s) in the sensed data).

Computer vision research (referred to as 'high-level' vision, see Havens & Mackworth (1983)) is usually concerned with top-down processing (Binford 1982). It can also be applied to aerial imagery to search for specific instances of, for example, houses in a suburban estate (see Nagoa & Matsuyama 1980; Matsuyama 1987) or in satellite imagery to monitor or track specific natural or anthropogenic features pre-extracted from maps, given a good camera model (see Tenenbaum *et al.* 1979).

Pattern recognition or image analysis research (referred to as 'low-level' vision, see Havens & Mackworth 1983) has usually been concerned with bottom-up processing such as line extraction (see Brown *et al.* (1983) for an example of a specialized feature detector known as a Hough transform) or region extraction (see Cross & Mason (1985) for an example of split-and-merge tactics) for later matching with a model pattern.

Whichever data or control flow is implemented, the most significant feature of image-understanding research is the inclusion of three-dimensional information based on the realization that it not only affects aerial photography (Herman & Kanade 1986) but, with increasing spatial resolution for satellite sensors, even orthographically projected *Landsat* images (see Justice *et al.* 1981; Woodham & Lee 1985).

Intrinsic image calculation refers to the extraction of depth, both relative (see, for instance, the 'shape-from' methods of Horn 1977) and absolute; the subsequent extraction of reflectance, an invariant physical quantity (to illumination and viewing conditions, see §3.3) by using depth and slope and, for a temporal sequence, motion estimates (for fluids, see §2) or change detection (see Tenenbaum *et al.* 1979). The resultant intrinsic images can then be segmented with a series of low-level operators to recover edges, regions and their spatial relations.

Three-dimensional analysis refers to the matching of features extracted from a combination of intensity and processed intrinsic-image features with instantiations of features extracted from the object and/or scene database. The former features will usually be referred to surface-based measurements and the latter will tend to be volume-based data. The objective of the scene data structures is therefore to convert volume representations to surface ones before 3D analysis. This may be accomplished by the incorporation of surface boundary information directly in volume representation schemes (see Chien & Aggarwal 1986).

Examples of this 3D analysis include map-image registration for the absolute orientation of *SPOT* data (Chevrel *et al.* 1981) with ground control points automatically extracted from digital map data (see Muller *et al.* 1987) and the quality assessment of digital elevation models (DEMs) derived from overlapping *SPOT* images (see Muller & Day 1987) with either manual photogrammetric measurements of geomorphometric features (e.g. ridges, stream networks) or DEMs derived from interpolated contours.

In the next three sections, examples are given of the recent development of some of these key components; in each, the role of knowledge sources and its multilevel invocation are shown.

3.2. *Knowledge sources and encapsulation*

These sources will include models of the image formation process; geometrical characteristics of objects within the scene and their interrelations (see Havens & Mackworth 1983); reflectance

characteristics of objects within a scene (see, for example, the DMA (U.S. Defence Mapping Agency) culture file description in Schachter 1980) and specialist expertise. This last source can be simplistically considered as consisting of two main types (see Reid *et al.* 1985): engineering models (e.g. of how oil is formed) and experiential 'rules of thumb' which can be readily combined into a set of rules for an expert system (e.g. applied to mineral prospecting, see Reid *et al.* 1985).

Knowledge encapsulation is still the most time-consuming and error-prone part of any image-understanding system. For example, digitization of paper maps, although automated for certain stages of the mapping process, is still very time-consuming and expensive (see discussion in Dowman & Muller 1986). Similarly, conversion of specialist knowledge into machine-readable rules is fraught with difficulties. For spatial information, attempts must be made to preserve the original accuracy of the data. Appropriate data structures to enable the integration of these multiscale data-sets are currently needed (see Jackson, this symposium).

An example of knowledge encapsulation studied here is raster to vector conversion, which may be required for the automated interpretation of satellite images of the oceans. Current semi-automated approaches rely upon use of the satellite orbital information and manual intervention to locate three or more ground control features (see Ho & Assem 1986). In the approach adopted here, automated edge detection is used to try to extract the coastline based

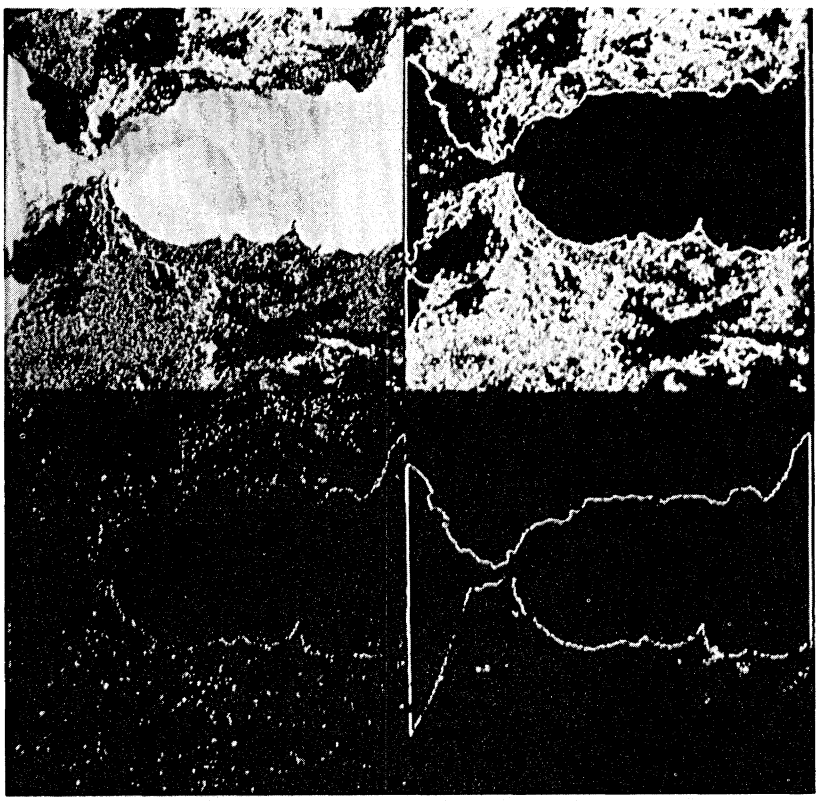

FIGURE 2. Example of automated coastline detection. The upper left figure shows the original daytime NOAA AVHRR image, with the upper right the application of edge detection using a Sobel filter. The lower left shows the application of a texture segmentation based on histogram thresholding of bimodal distributions of standard deviation of intensity within small window areas. The lower right shows the result of this edge-detection after the combination of the other two processes and erosion and dilation.

PHILOSOPHICAL TRANSACTIONS OF THE ROYAL SOCIETY A MATHEMATICAL, PHYSICAL & ENGINEERING SCIENCES

on gradients and differences in texture between the land, clouds and the sea. The target edge pixels are then connected by an iterative scheme of erosion and dilation (see Preston & Duff 1984). Figure 2 shows the results for a daytime NOAA AVHRR image of the Straits of Gibraltar.

Given a single successful segmentation, it was decided to apply this technique to several successive day and night images. Figure 3 shows the result compared with a digitized map of the area, which shows that the technique is quite robust for daytime images only. Hence, coastline detection must also rely on finding a unique set of correspondences between a

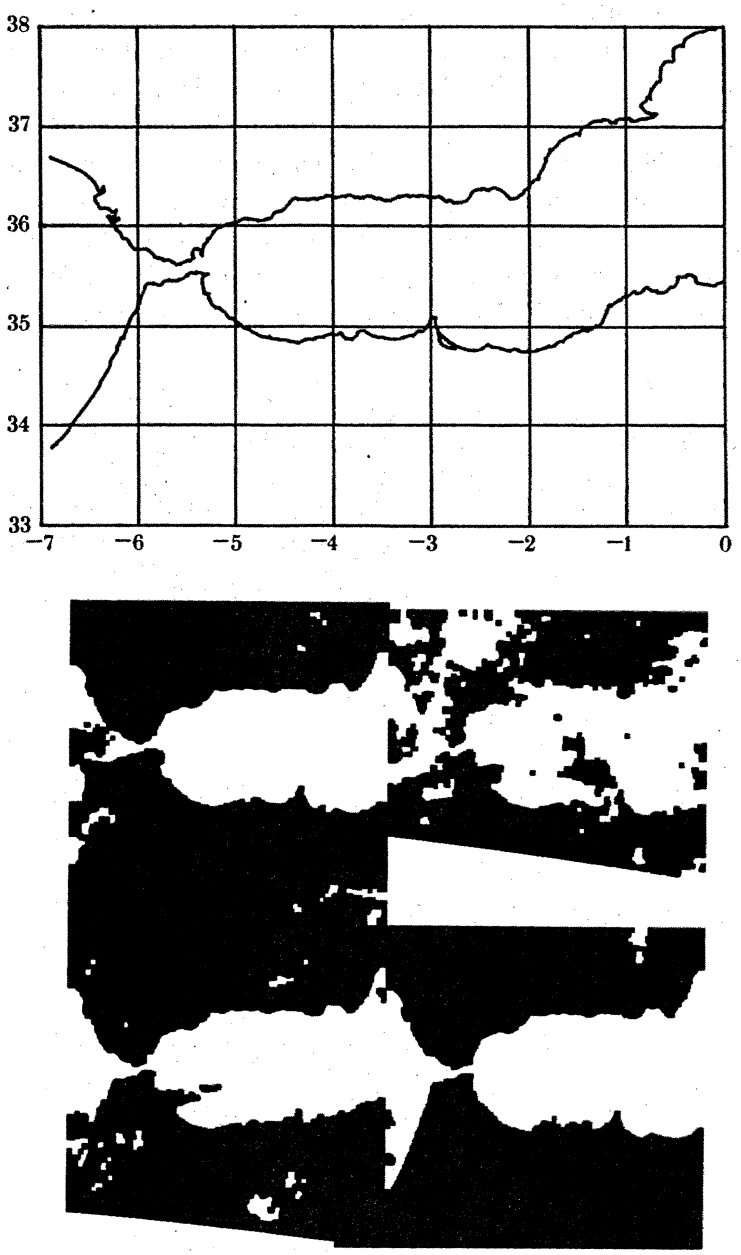

FIGURE 3. Example of the application of this coastline-detection technique to four sequential satellite images. The upper portion shows a digitized coastline supplied by NERC, and the lower portion shows the effect of applying this to two daytime and two night-time (upper right, lower left) images.

PHILOSOPHICAL TRANSACTIONS OF THE ROYAL SOCIETY A MATHEMATICAL, PHYSICAL & ENGINEERING SCIENCES

'perfect' model and noisy data. Fortunately, recent advances in dynamic programming (see Maitre & Wu 1986) indicate encouraging results in this area.

This example illustrates that several different types of knowledge source and encapsulation may need to be incorporated in automated processing, namely: platform and sensor models; digitized maps; distance metrics as cost function for the dynamic programming; physics (clouds are colder than land); and heuristics (sea is less textured than land).

3.3. *Models for image formation*

Figure 4 indicates schematically the primary sources of radiation received by a passive sensor onboard a satellite, ignoring the strong effects associated with the bidirectional viewing and illumination geometry (see Gerstl & Simmer 1986). It shows that to invert the signal received at the satellite to extract meaningful information on the reflectance properties of the surface cover will to a large extent depend on the relation between geometry and radiometry. Determining whether topography or surface cover dominates the signal received is one of the key issues in this area.

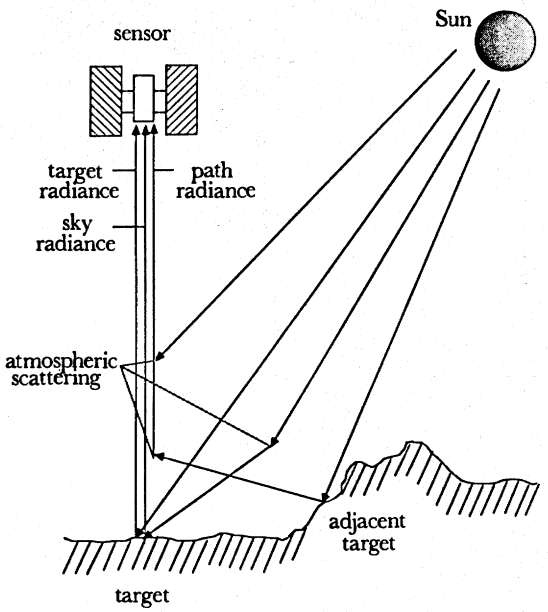

FIGURE 4. Some of the scattering processes involved in passive remote sensing at visible and near-infrared wavelengths (after Woodham & Lee 1985).

The techniques for modelling the effects of all the physical processes involved in scattering incident sunlight into a satellite sensor have recently been tackled with the advent of supercomputer-based simulation techniques. However, the atmospheric component can still be considered as intractable given the limited information available on the local distribution of water vapour and aerosol scatterers (see Pearce 1986 for an attempt to address this question by using mean climate data). Currently, only empirical methods can be used to assess the atmospheric components (path and sky radiance) of the signal (see Teillet 1986) in an attempt to remove their influence.

A simple shading model assuming lambertian reflectance can be applied to model the dominant effects of the surface shape (see Horn & Bachman 1978). Ray-tracing (see Fujimoto

PHILOSOPHICAL TRANSACTIONS OF THE ROYAL SOCIETY A MATHEMATICAL, PHYSICAL & ENGINEERING SCIENCES

et al. 1986) can then be used to investigate the effects of multiple scattering and variations in surface reflectance. Figure 5 shows an example of applying a simplified variant of ray tracing to a digital elevation model (DEM) by using just the first ray intersection to model cast and self shadows. The resultant areas which are in cast shadow can then be used in various schemes (see Teillet 1986) to estimate the effects of atmospheric scattering automatically. Surface geometries, such as tree canopies, may also be simulated by either image models (see Luttrell & Oliver, this symposium) or full stochastic models to allow ray scattering to stimulate surface bi-directional reflectance distribution functions (see Cabral *et al.* 1987).

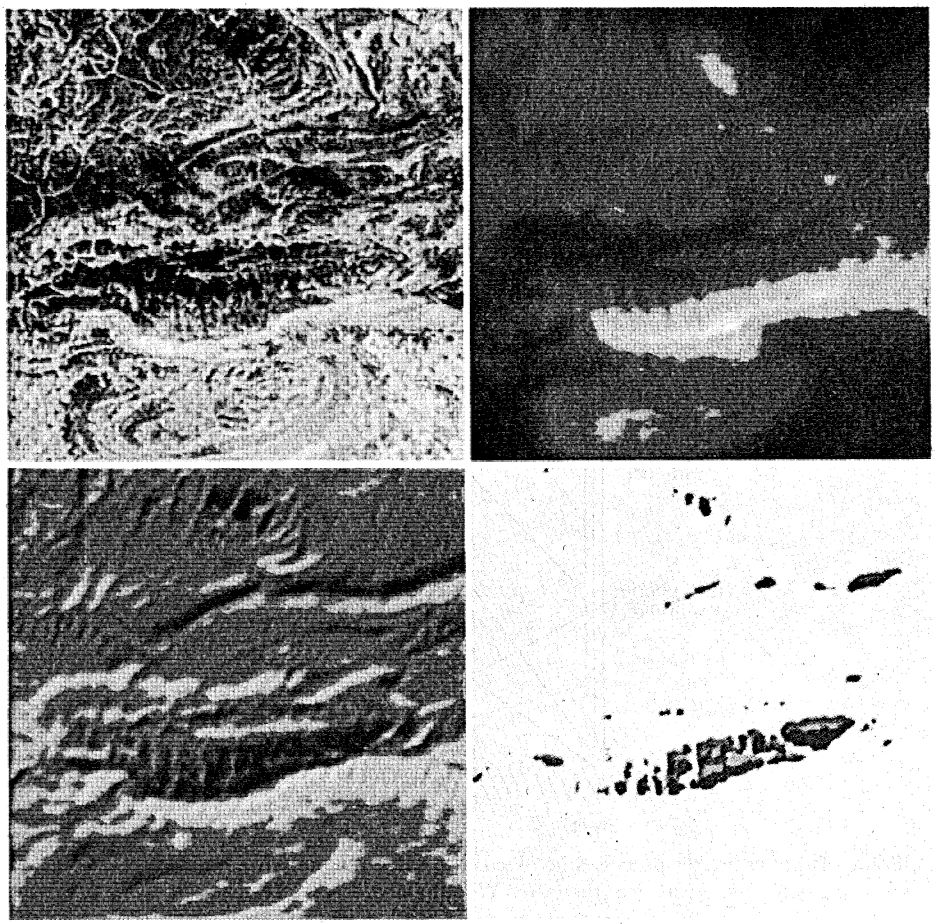

FIGURE 5. The generation of synthetic images for atmospheric correction is illustrated here. The upper left figure shows a small portion of a *SPOT* image (copyright, CNES) of 10 m resolution. The upper right shows an intensity range image of the DEM (corresponding digital elevation model); the lower left shows the simulation of the *SPOT* image with cast shadows included. The lower right shows those portions detected automatically which are in cast shadow that can be used for the correction of atmospheric effects.

These simulations of satellite images can also be used to develop better feature detectors, able to discriminate between effects due to relief and those due to variations in surface cover. Figure 6 shows an example of a comparison of the application of a zero-crossing filter to an original image (processed to 'remove' relief) with the cast shadow model. Developments of this kind may lead to a revolution in the way image processing operators can be developed, by simulating the known physics of the image formation before applying some appropriate heuristics.

PHILOSOPHICAL TRANSACTIONS OF THE ROYAL SOCIETY A MATHEMATICAL, PHYSICAL & ENGINEERING SCIENCES

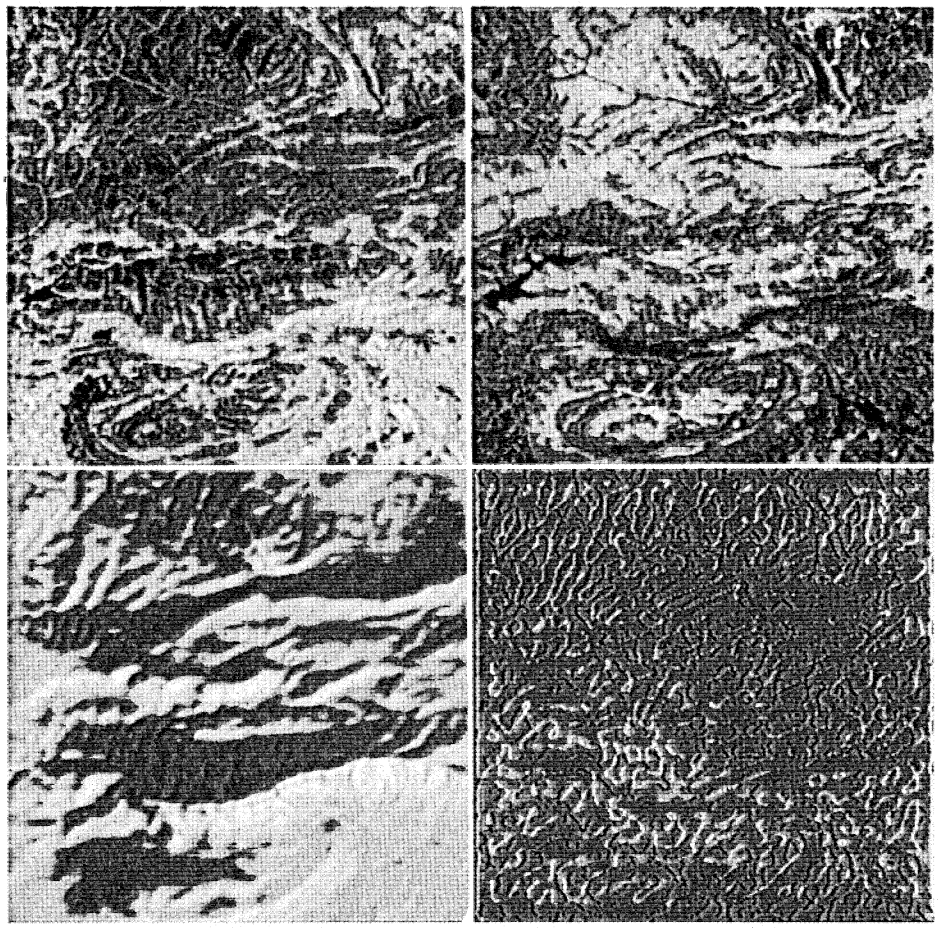

FIGURE 6. Application of synthetic image to the development of machine vision components. The upper left figure shows a *Landsat* band 7 image; the upper right shows a band ratio (band 3 : band 4) which tries to suppress effects of topography. The lower left figure is the same as the lower left in figure 5. Finally, the lower right figure shows the edges extracted from the synthetic image (in white) and those from the band ratio (in black).

This example again shows that several different types of knowledge need to be incorporated in automated processing, namely: platform and sensor models; digitized map data (from DEM creation); physics of image formation.

This technique is currently being tested for its routine application to satellite image processing when trying to detect oil and gas seepage-related events in surface reflectance (see Rock 1984) and for aiding geologists in their understanding of landscape processes in difficult terrain (see figure 7).

3.4. *Knowledge invocation*

Classical image understanding systems generally only try to introduce knowledge at high levels (e.g. object models, spatial relations between objects, see Besl & Jain (1985)) although there have been some recent attempts to introduce knowledge at low levels also (see Nazif & Levine 1984).

Little work, however, appears to have been done on trying to introduce knowledge at different levels explicitly. We will take two examples of our work: automated fluid motion measurement and automated stereo matching.

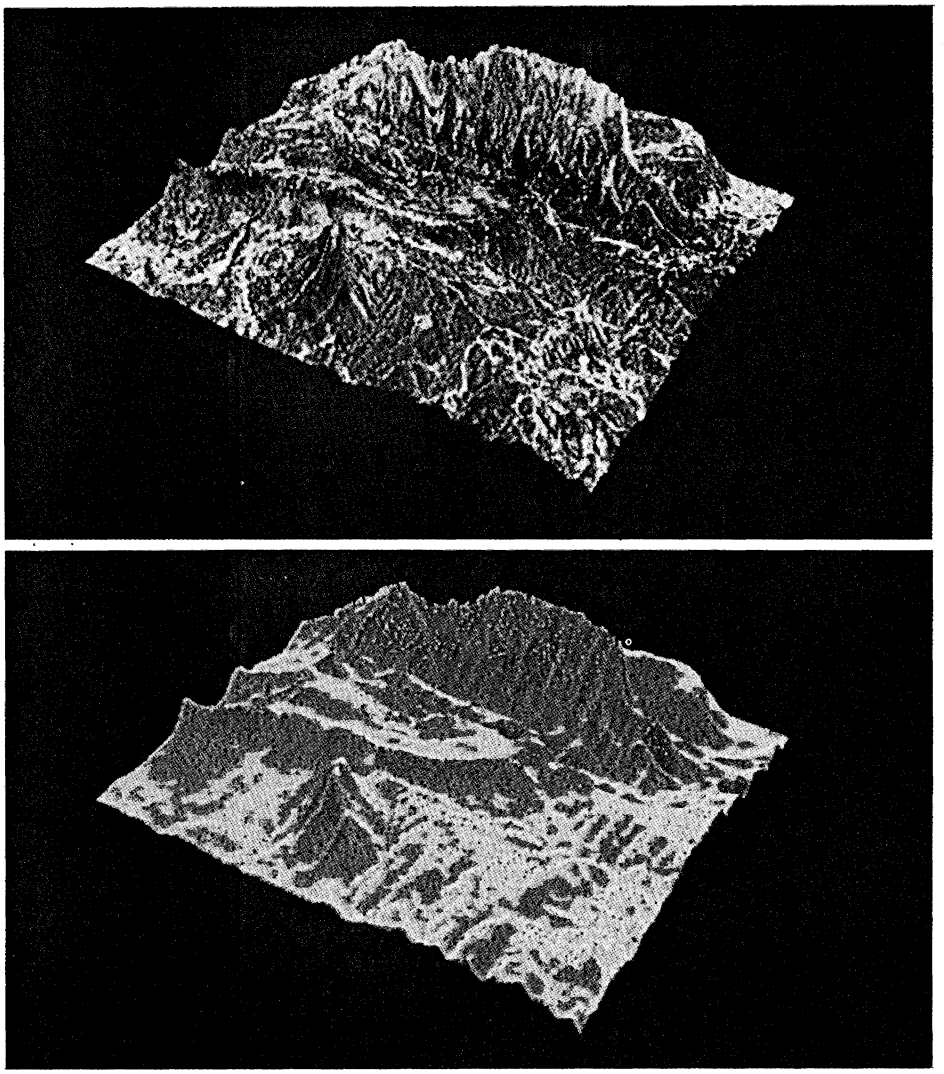

FIGURE 7. Perspective view of the area (Montagne Sainte Victoire in the South of France) with a *SPOT* image (upper) and a synthetic image, including cast shadow (lower) used to modulate the image intensity. Visualizations such as these may considerably aid the manual interpretation of areas by geologists.

Time sequences of satellite images have frequently been used to provide a visual impression of complex fluid dynamical processes. However, only crude techniques of cross correlation have so far been applied to meteorological (see Morgan 1979) or oceanographic (see Emery *et al.* 1986) satellite images.

Optical flow (see Horn & Schunck 1981) can be used for motion detection, although its original application was rigid-body motion. If u and v are the translational components of velocity, I the local image intensity and t, time,

$$uI_x + vI_y + I_t = 0. \tag{1}$$

Horn & Schunck present techniques for solving (1). A substantial modification that I introduced was to estimate a pixel velocity field by using cross correlation first (see figure 8 for the results) and use these estimates as initialization parameters for the Gauss–Seidel iterative solution.

PHILOSOPHICAL TRANSACTIONS OF THE ROYAL SOCIETY A MATHEMATICAL, PHYSICAL & ENGINEERING SCIENCES

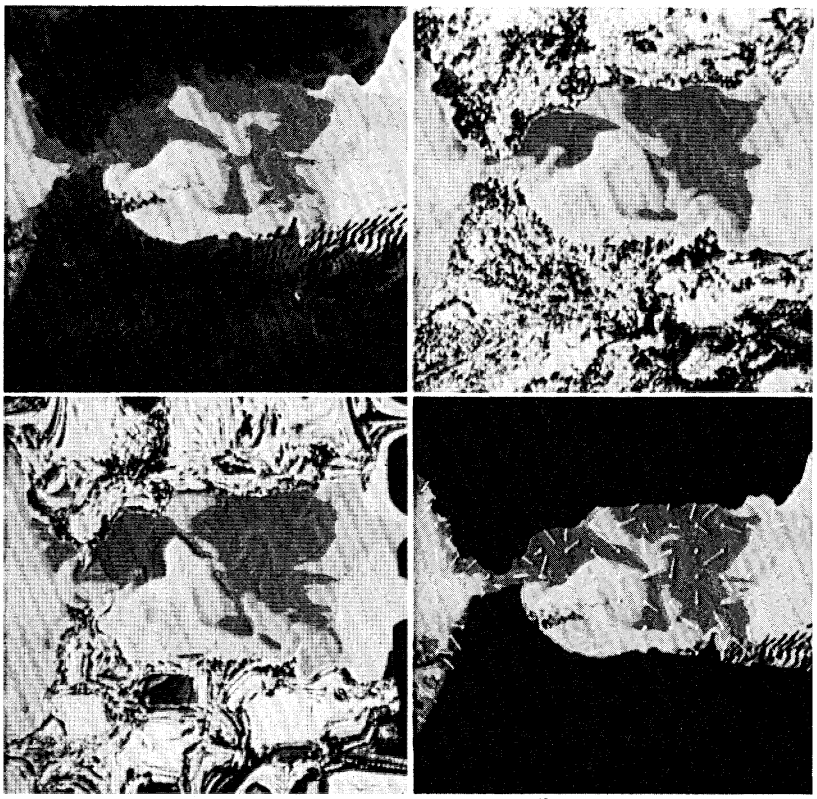

FIGURE 8. Example of optical flow applied to NOAA-AVHRR images. The upper figures show a daytime and night-time image; the lower right shows the velocities extracted automatically, averaged for 32-pixel windows. This type of eulerian velocity is directly compatable for immediate inclusion in numerical simulation. The lower left figure shows an attempt to verify the quality of the output by using the velocities to distort the second image with respect to the first, the resultant being a difference image, indicative of where the technique may be failing.

Equation (1) should be compared with a simple two-dimensional tracer conservation equation (see Stow 1985)

$$uC_x + vC_y - C_t = 0. \tag{2}$$

This similarity in the form of the equations may be used to introduce a process model into the image understanding system, subject to the physical constraints: for optical flow the pixel motion fields must be locally smooth; for tracer conservation, there must be no sources and sinks; and the intensity fields are representative of a conservative passive tracer (in this case, sea-surface temperature). This technique has been successfully applied to time sequences of satellite images of Jupiter from the *Voyager* spacecraft (see Muller 1982), and water-vapour images taken by *Meteosat*.

The second example concerns the automation of the extraction of three-dimensional coordinate information from the *SPOT* (see Muller *et al.* 1988), satellite, being performed within Alvey-funded project MMI/137 on *Real-time 2.5D vision systems*.

Figure 9 shows a schematic of the processing steps involved in extracting surface measurements of terrain (2.5D descriptions) automatically from overlapping *SPOT* images. Inspection of this figure shows a plethora of knowledge sources required: satellite ephemeris (platform parameters in figure 9), digital maps for ground control features (GCF in figure 9) used for

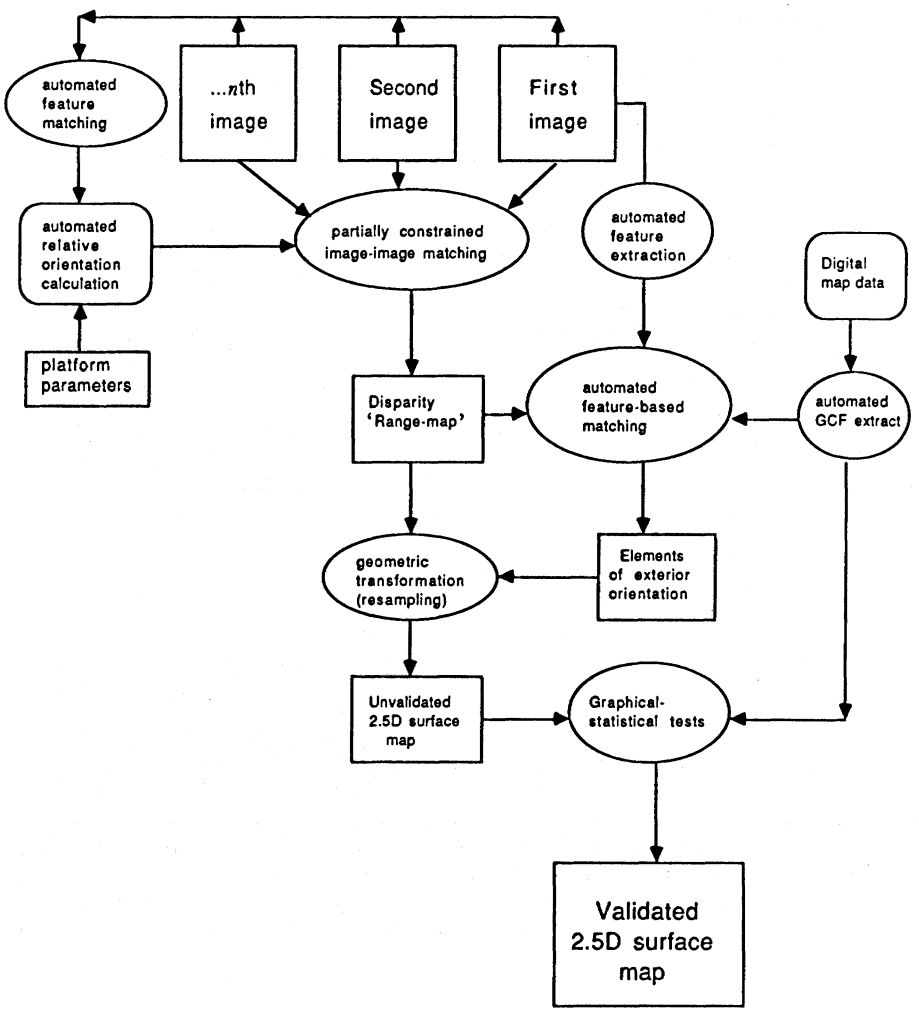

FIGURE 9. Flow-line model of automated stereo matching system for the automated generation of DEMs from *SPOT* images.

determining both the elements of exterior orientation and for validation that DEMs meet the target quality criteria; feature extractors optimized for *SPOT* topographic images and cost functions used for feature-based matching. The system is currently being implemented on a flexible parallel array of transputers (see figure 10) to enable processing of selected windows at video refresh rates.

4. CONCLUSIONS

In this paper, I have tried to indicate the reasons why a new approach to remote sensing is required if we are going to be able to process the flood of data promised by a new generation of satellite sensors (see Goetz *et al.* 1985) into meaningful information that can be incorporated into Geographical Information Systems (see Jackson, this symposium).

The complexity and difficulty of this task cannot be overstated, but current advances in image understanding research indicate which directions appear to be promising. A new era in remote sensing is dawning when quantitative analysis, based on image simulation, will be used

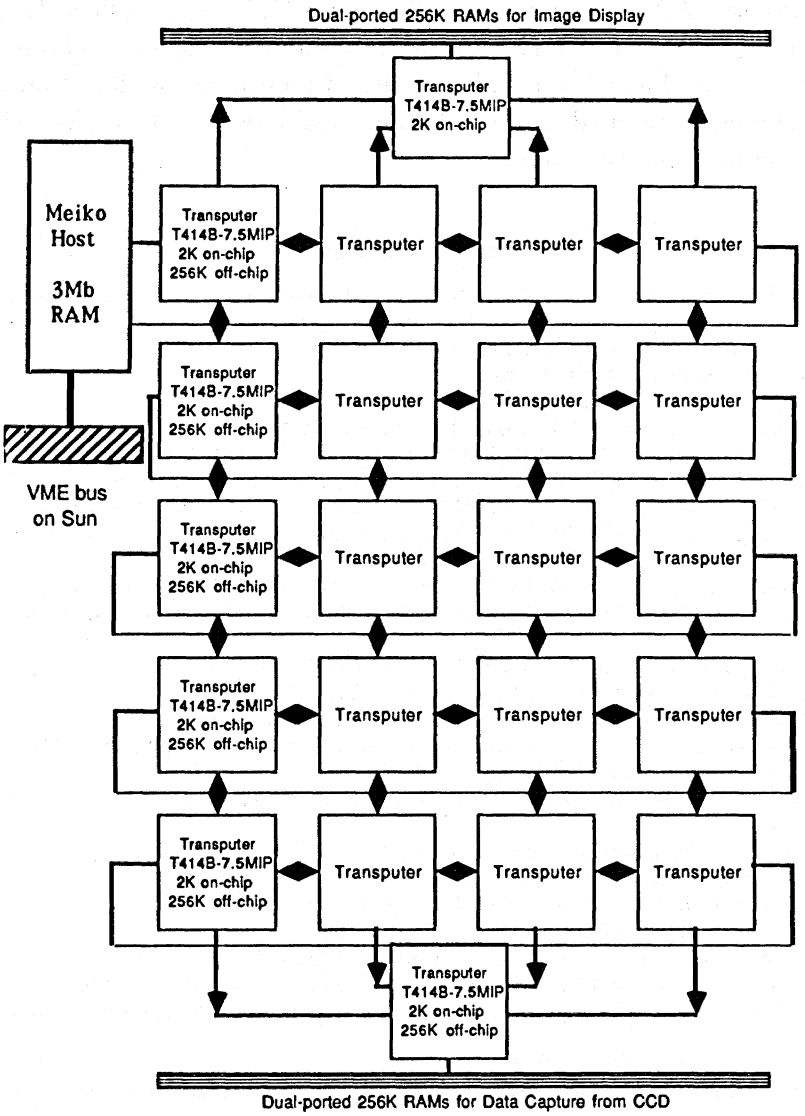

FIGURE 10. Schematic diagram of a transputer array being used at RSRE Malvern in developing a real-time 2.5D vision system for automatically extending DEMs from *SPOT* images.

to extract the information content automatically from satellite images in an analogous fashion to the interplay between theory and empiricism which has led to the successful development of numerical weather prediction.

I thank my students, particularly James Pearson and Philip Eales for providing some of the figures. Thanks also to Michael Dalton, for discussions on ray-tracing; Sam Richards and Tim Day for their work on terrain visualization; Paul Otto for discussions on DEM extraction; Ian Dowman for advice on photogrammetry; Kevin Collins, Brian Roberts, David Watson and Gordon Harp for giving me insight into understanding transputer networks; Mike Jackson, Alan Stevens, Andy Morris and Mark O'Neill for stimulating discussions on map–image matching; and Richard Clarke and Geoff Lawrence for advice on petrogeological applications. The research reported here is partly supported by SERC under the Alvey project number

MMI/137 (*Real-time 2.5D vision systems* (Participants: University College London (Departments of Photogrammetry and Surveying, and Computer Science); Thorn EMI Central Research Laboratories; Laser-Scan Laboratories, Cambridge; RSRE Malvern)); by BP Petroleum Development Limited and by the kind assistance of IBM UK Scientific Centre through their Visiting Scientist scheme.

References

Bernstein, R. 1986 In *Space science and applications: progress and potential* (ed. J. H. McElroy), pp. 71–76. New York: IEEE Press.
Besl, P. & Jain, R. 1985 *ACM Comput. Surv.* **17**, 75–145.
Binford, T. O. 1982 *Int. J. Robot. Res.* **1**, 18–62.
Bretherton, F. P. 1985 *Proc. IEEE* **73**, 1118–1127.
Brown, C. M., Curtiss, M. B. & Sher, D. B. 1983 In *Proc. 8th IJCAI*, pp. 1081–1085.
Cabral, B., Max, N. & Springmeyr, R. 1987 *ACM Comput. Graph*, **21**, 273–282.
Chevrel, M., Courtis, M. & Weill, G. 1981 *Photogramm. Engng Remote Sensing* **27**, 766–778.
Cross, A. & Mason, D. C. 1985 In *Proc. RSS/CERMA Int. Conf. on Advanced Technology for Monitoring and Processing Global Environmental Data, September 1985, London*, pp. 352–364.
Doyle, F. J. 1982 *Int. Arch. Photogrammie* **24**(1), 180–185.
Dowman, I. J. & Muller, J.-P. A. L. 1986 In *Proc. Auto-Carto London, 15–19 September 1986*.
Emery, W. J., Thomas, A. C., Collins, M. J., Crawford, W. R. & Mackas, D. L. 1986 *Eos, Wash.* **67**, 498–499.
Fujimoto, A., Tanaka, T. & Iwata, K. 1986 *IEEE Comput. Graphics Appl.* 16–26.
Gerstl, S. A. W. & Simmer, C. 1986 *Remote Sensing Environ.* **20**, 1–29.
Goetz, A. F. H., Rock, B. N. & Rowan, L. C. 1983 *Econ. Geol.* **78**, 573–590.
Goetz, A. F. H., Vane, G., Solomon, J. E. & Rock, B. N. 1985 *Science, Wash.* **228**, 1147–1153.
Havens, W. & Mackworth, A. 1983 *IEEE Computer* 90–96.
Herman, M. & Kanade, T. 1986 In *From pixels to predicates* (ed. A. P. Pentland), pp. 322–358. New Jersey: Ablex Publishing Corp.
Ho, D. & Assem, A. 1986 *Int. J. Remote Sensing* **7**, 895–904.
Horn, B. K. P. 1977 *Artif. Intell.* **8**, 201–231.
Horn, B. K. P. & Bachman, B. L. 1978 *Communs ACM* **21**, 914–924.
Horn, B. K. P. & Schunck, B. G. 1981 *Artif. Intell.* **17**, 185–199.
Jones, M. & Colombeski, N. C. 1981 *Int. J. Remote Sensing* **2**, 331–342.
Justice, C. O., Wharton, S. W. & Holben, B. N. 1981 *Int. J. Remote Sensing* **2**, 213–230.
Levine, M. D. 1978 In *Computer vision systems* (ed. A. R. Hanson & E. M. Riseman), pp. 335–352. New York: Academic Press.
Maitre, H. & Wu, Y. 1987 *Path. Recog.* **20**, 443–462.
Marr, D. 1982 *Vision: a computational investigation into the human representation and processing of visual information.* San Francisco: W. H. Freeman & Co.
Matsuyama, T. 1987 In *IEEE Trans. Geosci. Rom. Sens.* **GE-25**, 305–316.
McKeown, D. M. Jr., Harvey, W. A. Jr. & McDermott, J. 1985 *IEEE Trans. Pattern Analysis Mach. Intell.* **PAMI-7**, 570–585.
Morgan, J. 1979 *ESA Bull.* **20**, 14–16.
Muller, J.-P. A. L. 1982 Studies of Jovian meteorology using spacecraft and Earth-based images. Ph.D. thesis, University of London.
Muller, J.-P. A. L., Dowman, I. J., Day, T., Dalton, N., Paramananda, V., O'Neill, M. A., Morris, A. C., Stevens, A. & Jackson, M. J. 1987 In *Proc. Remote Sensing Society Conf., Nottingham, 7–11 September 1987*.
Muller, J.-P. A. L. & Day, T. 1987 In *Proc. Joint Photogrammetric and Remote Sensing Society Symposium, London, 11 November 1987*.
Muller, J.-P. A. L., Anthony, A., Brown, A., Chau, K. W., Collins, K. A. C., Dalton, N. M., Day, T., Deacon, A. T., Dowman, I. J., Ibbs, T. J., Jackson, M. J., Jobson, C., Montgomery, P. M., Morris, A. C., O'Neill, M. A., Otto, G. P., Paramananda, V., Recce, M., Robertson, G. W. R., Roberts, J. B. G., Stevens, A., Watson, D. M., Wilbur, S. 1988 First results from Alvey MMI-137. Real time 2.5D Vision Systems. *Int. J. Comput. Vision* (Submitted.)
Nagao, M. & Matsuyama, T. 1980 *A structural analysis of complex aerial photographs.* New York: Plenum Press.
NASA 1979 In *Proc. of the Large Area Crop Inventory Experiment (LACIE) Symposium.* NASA Johnson Space Center, JSC-16015.
Nazif, A. M. & Levine, M. D. 1984 *IEEE Trans. Pattern Analysis Mach. Intell.* **PAMI-6**, 555–577.
Pearce, W. A. 1986 *Appl. Opt.* **25**, 438–447.

PHILOSOPHICAL TRANSACTIONS OF THE ROYAL SOCIETY A MATHEMATICAL, PHYSICAL & ENGINEERING SCIENCES

Preston, K. Jr. & Duff, M. J. B. 1984 *Modern cellular automata*. New York: Plenum Press.
Reid, C. A., Fung, R. M., Tong, R. M. & Tse, E. 1985 In *Proc. IEEE 2nd Conf. on Artificial Intelligence Applications, 11–13 December 1985*, pp. 125–129.
Rock, B. N. 1984 In *Proc. Int. Symp. on the Remote Sensing of the Environment, 3rd Thematic Conference on Remote Sensing for exploration geology, Colorado Springs, April 16–19, 1984*.
Schachter, B. 1980 In *NATO Workshop on Map Data Processing* (ed. H. Freeman & G. Pieroni). New York: Academic Press.
Slama, C. C. (ed.) 1980 *Manual of photogrammetry*, 4th edn. American Society of Photogrammetry and Remote Sensing.
Stow, D. 1985 *Int. J. Remote Sensing* **6**, 1855–1860.
Swain, P. H. 1985 *Proc. IEEE* **73**, 1031–1039.
Tailor, A., Cross, A., Hogg, D. C. & Mason, D. C. 1986 *Image Vision Comput.* **4**, 67–83.
Teillet, P. M. 1986 *Int. J. Remote Sensing* **7**, 1637–1651.
Tenenbaum, J. M., Barrow, H. G., Bolles, R. C., Fischler, M. A. & Wolf, H. C. 1979 In *Proc. IEEE Workshop on Pattern Recognition in Image Processing, 6–8 August 1979, Chicago*, pp. 610–617.
Tenenbaum, J. M., Fischler, M. A. & Barrow, H. G. 1980 *Comput. Graph. Image Process.* **12**, 407–425.
Woodham, R. J. & Lee, T. K. 1985 *Can. J. Remote Sensing* **11**, 132–161.

Discussion

J. C. Scott (*A.R.E., Portland, Dorset, U.K.*). In the context of the data continuously available to the human being from his senses, the 2% quoted as processed from some satellites actually seems quite high. It is important to separate the customers and users of remote sensing into categories: those who need continuous global coverage at one end of the scale, and those needing occasional small regions at the other; immediacy of data is another factor. Would Dr Muller comment on how these factors affects the division between human interaction and automation?

J.-P. A. L. Muller. In the short term, human interaction will continue to play a key role in data analysis, even when guided by automated processing. An example of this that I showed was the visualization of terrain that could incorporate automatically generated DEMs.

In the longer term, human interaction will be involved in quality control of the output of an image-understanding system, both as it reaches intermediate conclusions and for final results.

S. Quegan (*Department of Applied and Computational Mathematics, The University, Sheffield, U.K.*). From the various examples quoted, can Dr Muller recognize any common elements, or does each problem have to be treated entirely in its own right?

J.-P. A. L. Muller. Common elements consist of the role of image-formation models, the multilevel invocation of multifarious knowledge sources and the matching processes needed for object–scene recognition. However, the type, quantity and quality of each knowledge source and when and where it is invoked is specific to a specialist domain application.

PHILOSOPHICAL TRANSACTIONS OF THE ROYAL SOCIETY A MATHEMATICAL, PHYSICAL & ENGINEERING SCIENCES

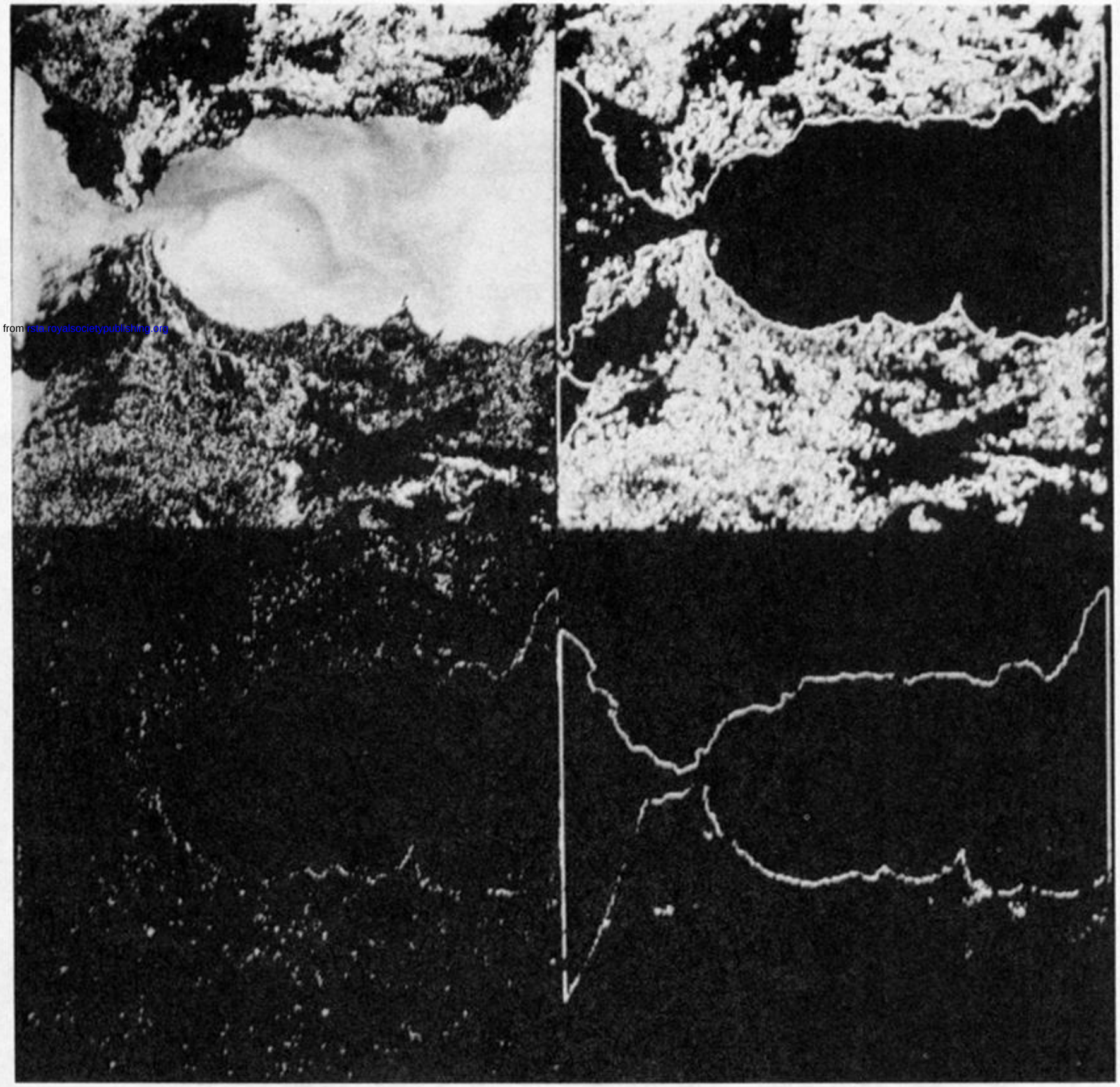

FIGURE 2. Example of automated coastline detection. The upper left figure shows the original daytime NOAA AVHRR image, with the upper right the application of edge detection using a Sobel filter. The lower left shows the application of a texture segmentation based on histogram thresholding of bimodal distributions of standard deviation of intensity within small window areas. The lower right shows the result of this edge-detection after the combination of the other two processes and erosion and dilation.

PHILOSOPHICAL TRANSACTIONS OF THE ROYAL SOCIETY A MATHEMATICAL, PHYSICAL & ENGINEERING SCIENCES
PHILOSOPHICAL TRANSACTIONS OF THE ROYAL SOCIETY A MATHEMATICAL, PHYSICAL & ENGINEERING SCIENCES

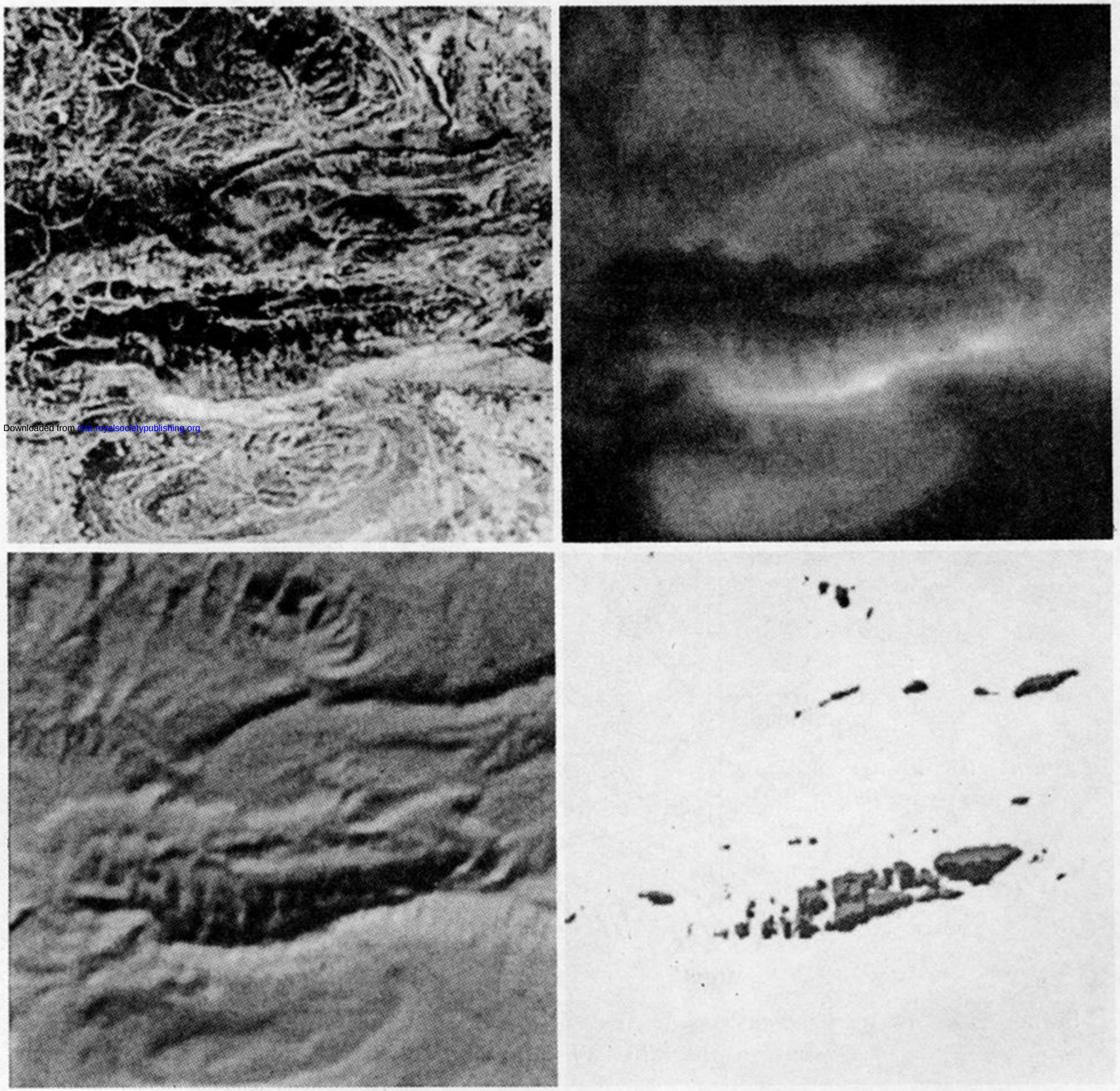

FIGURE 5. The generation of synthetic images for atmospheric correction is illustrated here. The upper left figure shows a small portion of a *SPOT* image (copyright, CNES) of 10 m resolution. The upper right shows an intensity range image of the DEM (corresponding digital elevation model); the lower left shows the simulation of the *SPOT* image with cast shadows included. The lower right shows those portions detected automatically which are in cast shadow that can be used for the correction of atmospheric effects.

PHILOSOPHICAL TRANSACTIONS OF THE ROYAL SOCIETY A MATHEMATICAL, PHYSICAL & ENGINEERING SCIENCES

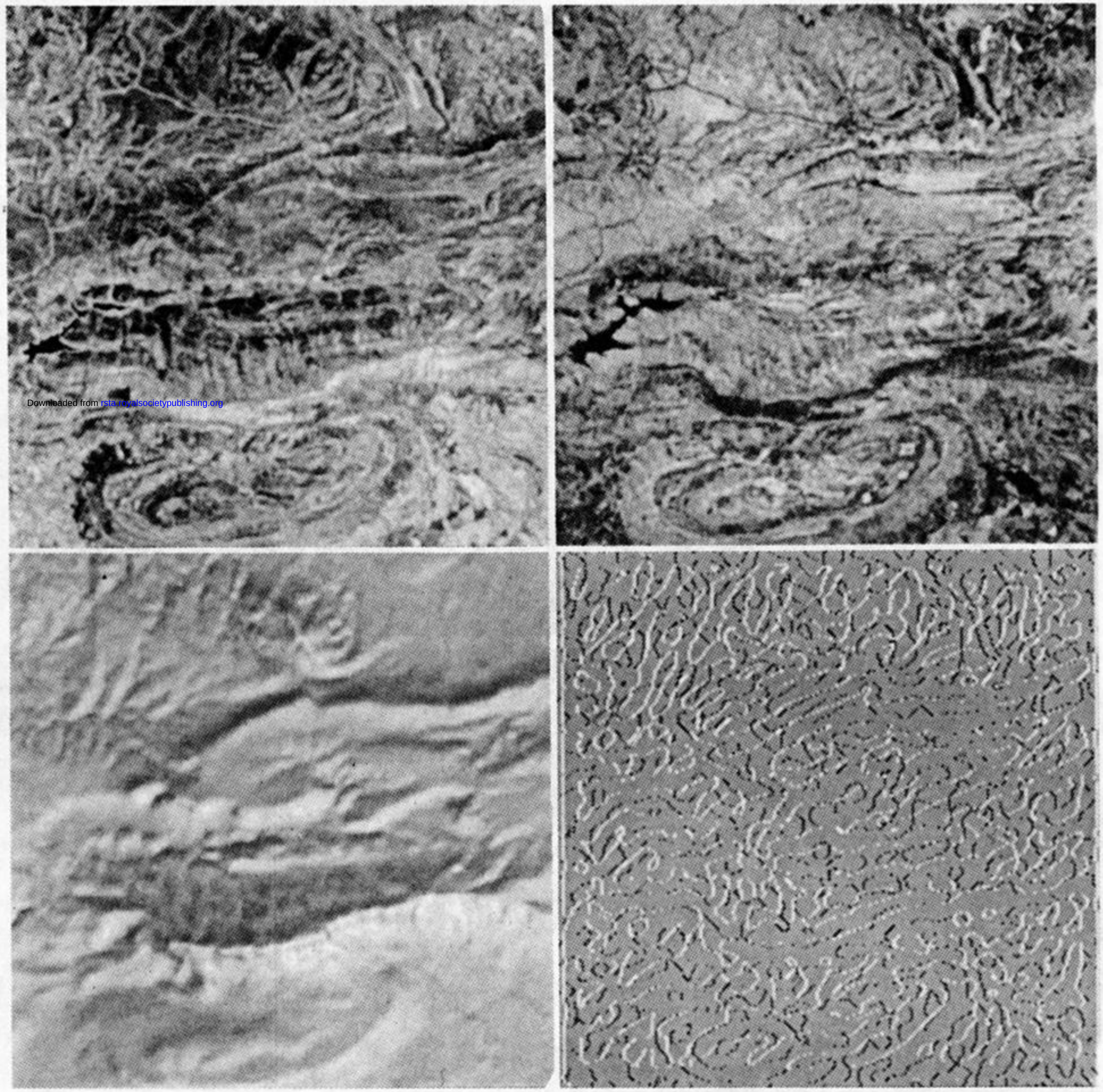

FIGURE 6. Application of synthetic image to the development of machine vision components. The upper left figure shows a *Landsat* band 7 image; the upper right shows a band ratio (band 3 : band 4) which tries to suppress effects of topography. The lower left figure is the same as the lower left in figure 5. Finally, the lower right figure shows the edges extracted from the synthetic image (in white) and those from the band ratio (in black).

PHILOSOPHICAL TRANSACTIONS OF THE ROYAL SOCIETY A MATHEMATICAL, PHYSICAL & ENGINEERING SCIENCES

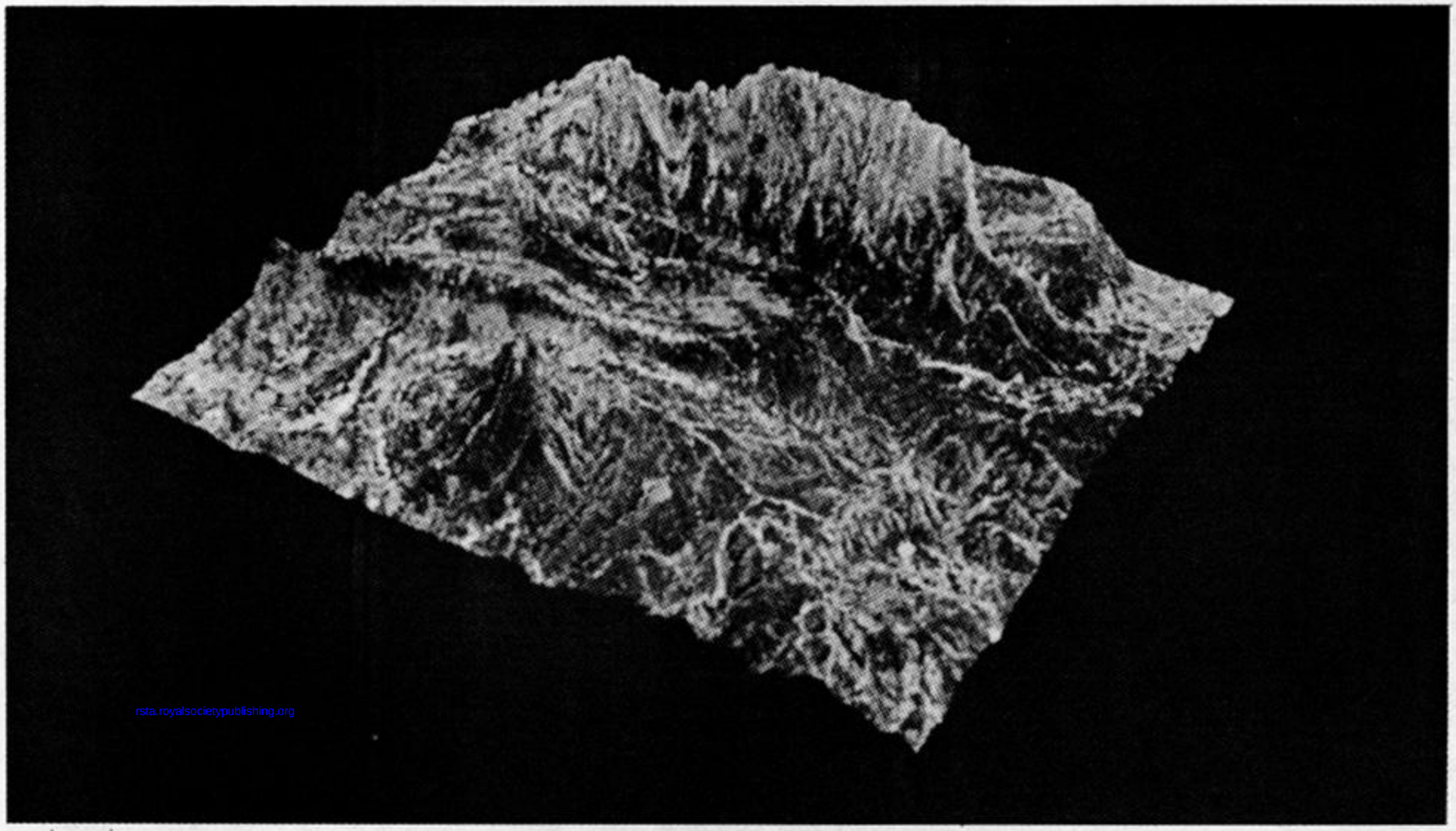

PHILOSOPHICAL TRANSACTIONS OF THE ROYAL SOCIETY A MATHEMATICAL, PHYSICAL & ENGINEERING SCIENCES

IGURE 7. Perspective view of the area (Montagne Sainte Victoire in the South of France) with a *SPOT* image (upper) and a synthetic image, including cast shadow (lower) used to modulate the image intensity. Visualizations such as these may considerably aid the manual interpretation of areas by geologists.

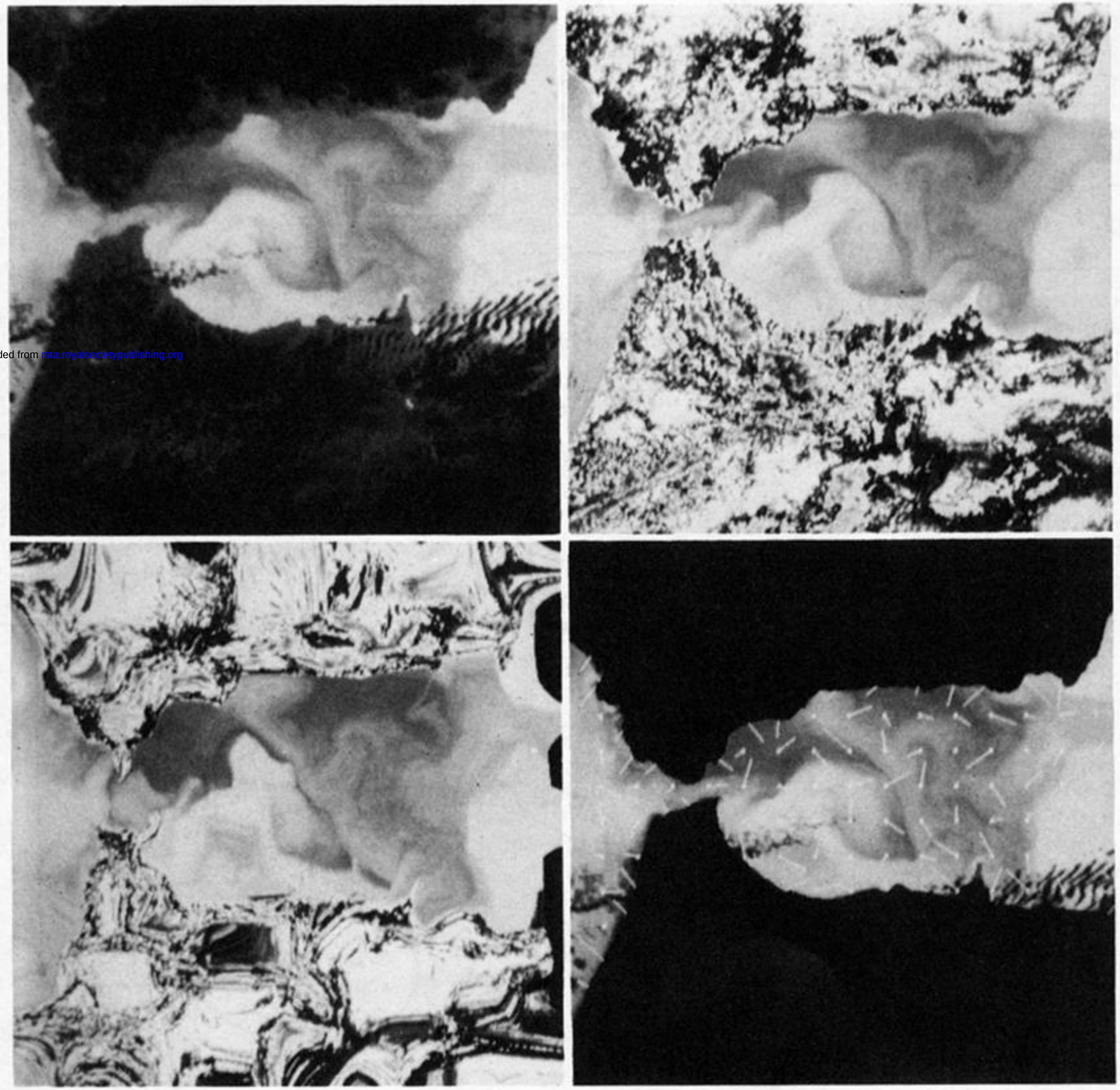

FIGURE 8. Example of optical flow applied to NOAA-AVHRR images. The upper figures show a daytime and nighttime image; the lower right shows the velocities extracted automatically, averaged for 32-pixel windows. This type of eulerian velocity is directly compatable for immediate inclusion in numerical simulation. The lower left figure shows an attempt to verify the quality of the output by using the velocities to distort the second image with respect to the first, the resultant being a difference image, indicative of where the technique may be failing.

PHILOSOPHICAL TRANSACTIONS OF THE ROYAL SOCIETY A MATHEMATICAL, PHYSICAL & ENGINEERING SCIENCES